Transportation
https://doi.org/10.1007/s11116-025-10673-y

Assessing the robustness of urban metro networks under flooding risk

Jie Li[1] · Ying Luo[1] · Jianghang Ou[1] · Suhua Zhou[1] · Chaoru Lu[2] · Yun Zhou[1]

Accepted: 10 August 2025

Abstract
Flooding poses a significant risk to urban metro networks, leading to station closures and service suspensions. By integrating the flood vulnerability of metro stations, this study evaluates the robustness of urban metro networks. Utilizing geographical, topological, and socio-economic data, the impact of flooding on the metro network is quantified. A composite index, which combines flood vulnerability with topological properties, is developed to evaluate the importance of individual stations under flood conditions. The Changsha metro network is analyzed as a case study, with simulations conducted to compare its performance in cascading and non-cascading failure scenarios. Three damage strategies—targeting stations based on degree centrality, flood vulnerability, and station importance—are applied to analyze network disruptions. Performance metrics, including the relative size of the largest connected subgraph (RS) and the network efficiency (NE), reveal varying degrees of network degradation under each damage strategy. The results show that stations such as Orange Isle Station and Xiangjiang Middle Road Station are highly susceptible to flooding. The network is most vulnerable to importance-based damage, with the removal of the top 6% of critical stations leading to a significant reduction in overall performance. These findings provide insights for enhancing urban metro network robustness, supporting station maintenance, and informing disaster prevention efforts.

Keywords Urban metro networks · Flood vulnerability · Robustness assessment · Cascading failures · Damage strategies

✉ Ying Luo
alychee0917@163.com

[1] College of Civil Engineering, Hunan University, Changsha, China

[2] Department of Built Environment, Oslo Metropolitan University, Oslo, Norway

Published online: 27 August 2025

Introduction

The accelerated urbanization and global warming have led to a rise in extreme rainfall events in many regions (Yang et al. 2021). These developments disrupt the natural water cycle in urban environments, further elevating the risk of urban flooding (Hallegatte et al. 2013). Metro systems, as vital components of urban transportation, are especially exposed to flooding risks due to their underground structure, complex interconnectivity, and high passenger density. China's metro systems have expanded rapidly in recent years. As of November 2024, China has 54 cities with a total of 313 urban rail transit lines in operation, covering 10,522.1 km. A total of 3.4 million train trips were made, carrying 2.71 billion passengers, a 5.2% increase year-on-year (China 2024). Nevertheless, their underground and confined structure makes them particularly susceptible to urban flooding risks (Lin et al. 2022a, b). Recent cases have underscored this vulnerability. On July 11, 2017, heavy rainfall in Paris caused the closure of 20 metro stations and the suspension of operations in some sections. On June 24, 2024, heavy rainfall in Changsha led to the full suspension of metro Line 2 and Line 3. Sudden events, such as intense rainfall, can disrupt the service of individual stations or network segments, potentially triggering cascading failures that may disable the entire system. As urban populations continue to rise and climate variability increases, the ability of metro networks to withstand and recover from such disruptions has become a critical concern for urban planning and disaster risk management.

Despite the growing relevance of these risks, current research on metro network robustness tends to focus either on topological indicators or general operational metrics. Most studies simulate cascading failures based on overload redistribution or topological attacks but rarely integrate flood vulnerability data or real-world environmental hazards into the robustness evaluation framework. Moreover, limited attention has been paid to how station-level flood susceptibility, shaped by geographic and socio-economic factors, interacts with network topology to influence cascading dynamics. This presents a significant research gap, particularly in flood-prone regions where metro systems are both lifelines and high-risk assets.

This study proposes a comprehensive robustness evaluation framework that incorporates both network structure and flood vulnerability under disruption scenarios. The goal is to better understand how flood-induced disruptions propagate through metro networks and how system resilience can be improved through informed planning and risk mitigation. The primary contributions of this study are as follows:

(1) A method is proposed to quantify the flood vulnerability of metro stations based on geographic, topological, and socio-economic data. This approach uses the entropy method and Technique for Order Preference by Similarity to an Ideal Solution (TOPSIS) to assess station importance, incorporating the topological properties of network nodes.
(2) A load redistribution-based cascading failure model is proposed to quantitatively evaluate the robustness of urban metro networks when subjected to various damage. The analysis applies two robustness assessment metrics: the network efficiency (NE) and the relative size of the largest connected subgraph (RS).

The structure of the paper is outlined as follows: Sect. "Literature review" presents a detailed description of the proposed methodology. Sect. "Methodology" applies the developed model

to the Changsha metro network and analyzes the findings. In conclusion, Sect. "Case study" summarizes the findings of the study and suggests possible directions for future research.

Literature review

Previous studies have explored metro network robustness from multiple perspectives, focusing on structural and functional metrics, modeling and assessment of cascading failures, design of targeted disruption strategies, and the impact of environmental factors (e.g., flooding).

Network robustness is defined as the ability of a network to maintain its essential functions and operational efficiency under various disruptions (Yin and Wu 2023; Zhang et al. 2024, 2019). Simulated disruptions and associated performance metrics are commonly used for assessment. Metrics for assessing metro network robustness can be broadly classified into topological and operational categories. Topological metrics analyze the structural characteristics of the network, evaluating its connectivity and the interactions between nodes and edges under disruptions. Topological metrics focus on analyzing the structural characteristics of metro networks and their connectivity under disruption scenarios. For example, Yu et al. (2019) employed three metrics—network connectivity efficiency, the size of the largest connected subgraph, and average subgraph size—to assess the robustness of the Nanjing metro network under random and targeted damage. Mussone et al. (2024) assessed network robustness by employing the Sum of Weighted Distances Index (SWDI) to analyze and measure changes in traveled distances. The SWDI quantifies the percentage change in travel distances when a node and all its associated edges are disrupted. Operational metrics focus on the functional aspects of the network, assessing its ability to continue providing services despite disruptions. Ma et al. (2020) introduced a method for assessing metro network vulnerability, incorporating metrics such as average shortest path, passenger flow intensity, and congestion indicators.

Cascading failures is a key manifestation of system vulnerability when the network structure or function is disrupted. Cascading failures occur as the failure of a node or link initiates a chain reaction, leading to subsequent failures caused by redistributed overload (Motter and Lai 2002). This phenomenon is prevalent in transportation networks, where the failure of high-load nodes and/or links can lead to the collapse of the entire network. Thereby, the robustness and vulnerability of transportation systems has often been studied after cascading failures (Huang et al. 2021; Lu et al. 2022; Yang et al. 2022; Yin et al. 2022). Shen et al. (2024) proposed a cascading failure model incorporating node load and passenger behavior to examine the vulnerability of metro networks. Wang and Tian (2021) adopted a weighted composite index, combining demand loss and travel time delays during cascading failures, to assess the robustness of metro networks. Li et al. (2024) utilized an enhanced Coupled Map Lattice (CML) model to simulate cascading failures in metro networks, incorporating factors such as station centrality, geographic elevation, and passenger flow dynamics. This approach offers a comprehensive understanding of how these elements interact and contribute to network vulnerabilities.

In terms of disruption targeting, existing studies often select network nodes or edges as disruption objects, with the disruption sequence determined by their topological metrics. Current studies often rank nodes or links by calculating topological metrics such as degree

centrality and betweenness centrality, to determine damage strategies (Frutos Bernal et al. 2019; Liu et al. 2021; Mouronte-Lopez 2021; Qi et al. 2022). Yang et al. (2015) proposed a method combining node degree and betweenness to address the limitation of single-factor approach for assessing node importance. Some studies also incorporate station operational conditions and environmental factors, along with topological metrics, to provide a more comprehensive assessment of metro station importance. For instance, Ma et al. (2023) ranked stations in the Xi'an metro network under cascading failure scenarios based on metrics like the passenger flow loss rate, the node centrality, and the network efficiency loss rate. Zhang et al. (2024) described station importance in urban metro networks based on the station evacuation capacity and passenger volume. Studies on targeted damage strategies often simulate network damage under extreme conditions to determine damage sequences. Two approaches are prevalent: one considers changes in network functionality when nodes fail due to overload, while the other analyzes node vulnerability to define failure probabilities. Khazeiynasab and Qi (2021) analyzed the sequence of events to study the resilience of power systems under extreme temperatures. Dong et al. (2019) determined the sequence of targeted damage based on road damage probabilities and assessed network robustness in terms of the connectivity of critical nodes.

Beyond structural and functional factors, environmental disruptions, especially flood risk, should also be considered in metro network robustness studies. Flooding can simultaneously disable multiple stations and lines, triggering large-scale cascading failures. Flood vulnerability indicators are well-developed by researchers using geographical factors, including slope and precipitation (Li et al. 2023; Lyu et al. 2018; Ma et al. 2021). These geographical factors are fundamental, but recent studies have expanded the scope to consider a broader range of elements. Additionally, Wang et al. (2024a, b) incorporated economic and social factors and applied the Light Gradient Boosting Machine (Light GBM) model to analyze flood vulnerability. After determining the assessment indices, various methods are employed to assign weights, including both subjective and objective weighting approaches (Cabrera and Lee 2020; Mahmoodi et al. 2023; Roopnarine et al. 2022). Diriba et al. (2024) used the Analytic Hierarchy Process (AHP) to determine indicator weights and then incorporated remote sensing with GIS technologies to analyze regional disaster risk. Chen et al. (2023) integrated the AHP and the entropy method to evaluate urban flood vulnerability. Wang et al. (2024a, b) proposed nine flood risk-related indicators encompassing hazard, exposure, and vulnerability, and then applied the entropy method and Euclidean distance to estimate the flood risk. This integrative method considers both environmental and social dimensions, offering a more holistic assessment method of flood risk.

Most previous studies on targeted network damage determine damage order based on topological properties, such as degree centrality. This approach may limit the accuracy of robustness assessments for metro networks, as it fails to account for practical operational and environmental influences on network functionality. Studies on network robustness have primarily focused on evaluating the resilience of road transportation systems under extreme scenarios, such as natural disasters. However, studies specifically examining the effects of flood-related cascading failures within urban metro networks remain limited. Floods can severely impact metro systems by causing cascading breakdowns across multiple stations and lines, seriously affecting the efficiency of urban transportation operations. Therefore, considering flood risk when studying the robustness of metro networks holds practical significance. So this study expands upon existing network resilience models by incorporating

traditional topological properties (e.g. network efficiency) and performance indicators (e.g. passenger flow). By considering the specific impacts of urban flood risk on urban metro networks, this study provides a more comprehensive framework for assessing metro system robustness.

Methodology

Flood vulnerability assessment

Assessment indicators

This study applies the Airlie House Vulnerability (AHV) model (Turner et al. 2003) to define the vulnerability of metro stations under urban flooding scenarios. The analysis considers the susceptibility of metro stations and passengers to flood impacts, focusing on three aspects: exposure to flood hazards, sensitivity to disaster factors, and the adaptive capacity to recover from flood events. Based on indicators illustrated in Fig. 1, the flood vulnerability of metro stations was assessed across three aspects: exposure, sensitivity, and adaptability.

Exposure indicators capture the potential impact of flooding on metro stations in terms of passenger flow (Rafiul et al. 2023), the number of entrances and exits (Lyu et al. 2019), the density of nearby schools, and the proportion of vulnerable populations (Wang et al. 2024a, b). High passenger flow exacerbates flooding by increasing the load on stations and surrounding areas, while reducing the effectiveness of flood control measures. Entrances and exits serve as interfaces between the internal and external environments of buildings. During rainfall, particularly intense or sustained precipitation, rainwater may infiltrate the interior of buildings through these openings. An increase in the number of entrances and exits provides more pathways for rainwater to enter the building, thereby elevating the risk

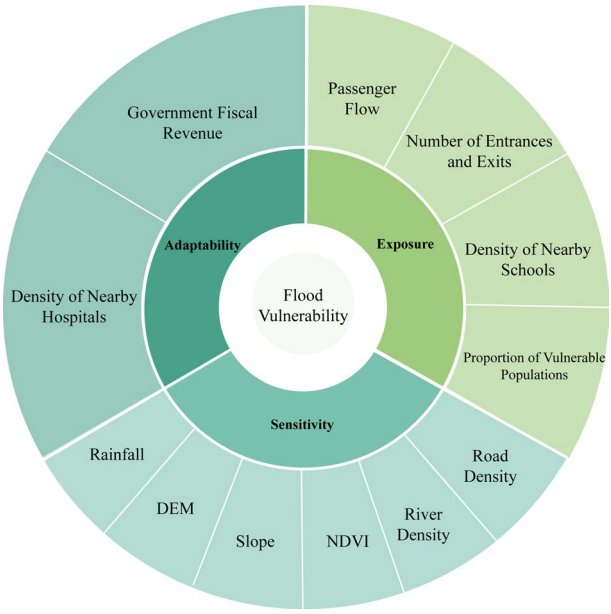

Fig. 1 Indicators for flood vulnerability assessment

of water infiltration. The concentration of schools in the area intensifies safety concerns, as flooding could interfere with the commuting and safety of students, teachers, and parents. Additionally, vulnerable groups, including children and the elderly, are more susceptible to the impacts of disasters and face heightened risks.

Sensitivity indicators evaluate the influence of environmental and geographical factors on metro stations, encompassing rainfall (Chen et al. 2014), Digital Elevation Model (DEM) (Hoque et al. 2019), slope (Sahu 2014), Normalized Difference Vegetation Index (NDVI) (Sar et al. 2015), river density (Roy et al. 2021), and road density (Guan et al. 2024). Excessive rainfall, particularly in areas with poor drainage systems, exacerbates waterlogging and backflow risks. Low elevations (Tayyab 2021) and gentle slopes (Hamidi et al. 2020) around stations increase flood susceptibility by facilitating water accumulation, while higher slopes enable faster runoff. Dense vegetation mitigates runoff and helps manage flood risks, whereas high river and road densities elevate the likelihood of flooding through rapid water level rises and limited absorption of rainwater.

Adaptability indicators focus on the capacity of metro stations to manage and recover from flooding, factoring in local government fiscal revenue (Duan et al. 2022) and the density of nearby hospitals (Pu et al. 2024). Higher fiscal revenue reflects greater economic resources for disaster preparedness, efficient response, and robust flood prevention infrastructure. The presence of hospitals within proximity enhances emergency response efficiency, ensuring timely evacuation and medical support during flooding events. These exposure, sensitivity, and adaptability indicators provide a comprehensive framework.

Assessment method

Due to the varying scale of different assessment indicators, direct comparison was challenging. To tackle this issue, the indicators were normalized using consistent methods, thereby removing any dimensional discrepancies. Indicators were classified into two categories: positive and negative (refer to Fig. 2). For positive indicators, higher values represent increased flood vulnerability, while for negative indicators, higher values signify reduced flood vulnerability. The normalization formulas used are as follows (Wu et al. 2021):

$$r_{ij}^{p} = \frac{x_{ij} - x_j^{min}}{x_j^{max} - x_j^{min}} \tag{1}$$

$$r_{ij}^{n} = \frac{x_j^{max} - x_{ij}}{x_j^{max} - x_j^{min}} \tag{2}$$

Fig. 2 Indicator categories for flood vulnerability assessment

where r_{ij}^{p} represents the *i*th value of the *j*th positive assessment indicator (i = 1, ..., m; j = 1, ..., n), r_{ij}^{n} denotes the *j*th value of the *j*th negative assessment indicator. Where x_j^{max} represents the maximum value of the *j*th indicator, and $x_j^{\min}$ denotes the minimum value of the *j*th indicator.

The entropy method (Zhang et al. 2023) effectively reflects the importance of each indicator through its distribution characteristics. It assigns weights to indicators based on the dispersion of their data values. Compared with subjective approaches, the entropy method reduces human bias by deriving weights objectively. Indicators with greater variability contain more information and are given higher weights, while indicators with low variability are assigned lower weights. Lower entropy indicates stronger discriminative ability and results in a higher weight. The entropy method provides a more comprehensive representation of the interconnections between various dimensions of urban form disaster vulnerability. Thus, this method is employed to determine the relative weight of different factors influencing the flood vulnerability of metro stations. To begin, the target matrix $R = (r_{ij})_{m\times n}$, representing m evaluation objects and n evaluation indicators, is normalized using Eqs. (1) and (2). The weight ω_j is calculated through the following equations:

$$\begin{cases} e_j = -K \cdot \sum_{i=1}^{m} p_{ij} \ln p_{ij} \\ p_{ij} = \frac{r_{ij}}{\sum_{i=1}^{m} r_{ij}}, i = 1, ..., m; j = 1, .., n \\ K = \frac{1}{\ln m} \\ E_j = 1 - e_j \\ \omega_j = \frac{E_j}{\sum_{j=1}^{n} E_j} \end{cases} \tag{3}$$

where p_{ij} represents the weight of the *i*th object relative to all objects under the *j*th indicator. A positive constant K is introduced to ensure that $0 \le e_j \le 1$ is the number of assessment objects. The constant K serves solely as a unit of measurement. e_j denotes the entropy value of the *j*th indicator, while ω_j represents its corresponding weight.

The weight vector of the evaluation indicators $W = (\omega_1, \omega_2, ..., \omega_n)$ can be obtained through the calculations described above. The calculation of the weight vector facilitates the subsequent application of TOPSIS analysis for evaluating and ranking alternatives. TOPSIS (Majumdar et al. 2020) is a multi-criteria decision-making method that assesses and ranks alternatives by measuring their closeness to the ideal solution and their distance from the negative ideal solution. This method integrates all indicators to provide a comprehensive score for the assessed object. TOPSIS was applied to integrate the weighted indicator values and assess flood vulnerability for each station.

The steps of the TOPSIS method are as follows:

(1) Weighted Scoring
The weighted scoring matrix is calculated by combining the target matrix $R = (r_{ij})_{m\times n}$ with the weight vector W of the evaluation indicators, as shown in Eq. (4):

$$Z = (z_{ij}) = (r_{ij} * \omega_j) \tag{4}$$

(2) Construct Positive and Negative Ideal Solutions

The positive ideal solution Z^+ is a vector composed of the maximum values of each column in the weighted scoring matrix Z, while the negative ideal solution Z^- consists of the minimum values of each column in Z. The formulations for Z^+ and Z^- are shown in Eqs. (5) and (6), respectively:

$$Z^+ = \left(z_1^+, z_2^+, ..., z_n^+\right) \tag{5}$$

$$Z^- = \left(z_1^-, z_2^-, ..., z_n^-\right) \tag{6}$$

(3) Calculate the Distances to the Ideal Solutions.
The distances of each evaluation object from both the positive and negative ideal solutions are calculated using Eqs. (7) and (8), respectively:

$$d_i^+ = \sqrt{\sum_{j=1}^{n} \left(z_j^+ - z_{ij}\right)^2} \tag{7}$$

$$d_i^- = \sqrt{\sum_{j=1}^{n} \left(z_j^- - z_{ij}\right)^2} \tag{8}$$

(4) Calculate the TOPSIS Scores for Each Object.
The TOPSIS score for each evaluation object is calculated using Eq. (9), as demonstrated below:

$$s_i = \frac{d_i^-}{d_i^- + d_i^+} \tag{9}$$

Topology network construction

In complex network analysis, three primary methods exist for constructing network topologies: the Space-L, Space-P, and Space-R methods. The Space-L method is based on the principle that if two nodes are adjacent on the same line, they are directly connected by an edge. This method accurately reflects the adjacency relationships between subway stations and the alignment of subway lines. This is crucial for analyzing the robustness of the metro network and facilitates the calculation and analysis of its key characteristics. In contrast, the Space-P method may overlook direct connections between adjacent stations, while the Space-R method lacks widespread recognition and application in subway network construction. Consequently, this study utilized the Space-L approach to construct the topological network structure.

Network topological metrics

Analyzing the structural properties of a network is essential for comprehending its functionality, resilience, and vulnerability, especially when considering metro networks. Topological metrics provide quantitative tools to assess various aspects of a network's structure and behavior, enabling a comprehensive evaluation of its performance and robustness. Existing

studies commonly utilize metrics such as degree and betweenness, as shown in Table 1. These metrics offer valuable insights into the roles of individual nodes and the network's overall stability. Therefore, these metrics are also involved in this study.

(1) Degree and Degree Centrality.
The degree of a node represents the number of links between a station and other stations. A higher node degree corresponds to a greater degree centrality, indicating the node's significance within the network. The degree of a node is calculated using Eq. (10), while the degree centrality is computed using Eq. (10):

$$C_k(i) = \frac{\sum a_{ij}}{N-1} \tag{10}$$

where $a_{ij} = 1$ indicates that the node i is directly connected to the node j; otherwise,$a_{ij} = 0$; $N-1$ signifies the theoretical maximum number of connections that the node i could establish with all other nodes in the network.

(2) Betweenness and Betweenness Centrality.
Betweenness quantifies the number of shortest paths in a network that pass through a specific node. A station with more shortest paths passing through it has a higher betweenness value, reflecting its greater importance and influence within the network. The betweenness centrality of a node is calculated using Eq. (11), as follows:

$$C_B(i) = \frac{1}{(N-1)(N-2)/2} \sum\nolimits_{m \neq i \neq n} \frac{\sigma_{mn}(i)}{\sigma_{mn}} \tag{11}$$

where σ_{mn} represents the total number of shortest paths between the node m and the node n, while $\sigma_{mn}(i)$ indicates the number of those paths that pass through the node $m(m \neq i \neq n \& 1 \leq m < n \leq N)$.

(3) Shortest Path Length.
In urban metro networks, the shortest path length is the path that connects these two nodes with the least number of edges. The average shortest path length represents the mean value of the shortest distances between all station pairs. The calculation method is provided in Eq. (12).

$$L = \frac{\sum_{i \neq j} l_{ij}}{N_d} \tag{12}$$

where N_d denotes the total number of nodes in the network, and l_{ij} represents the shortest path distance between the node i and the node j.

Table 1 Topological metrics of changsha metro network

Topological metrics	Sources
Degree and degree centrality	Pei et al. (2024) and Huang et al. (2024)
Betweenness and betweenness centrality	Xu et al. (2019) and Chen et al. (2024)
Shortest path length	H. Lin et al. (2022a, b)
Clustering coefficient	Hieu et al. (2019)

(4) Clustering Coefficient.
The clustering coefficient of a node is the ratio of the actual number of edges between its neighbors to the maximum number of edges that could potentially connect them. Its calculation is provided in Eq. (13):

$$V_i = \frac{E_i}{k_i(k_i - 1)/2} \tag{13}$$

where E_i represents the actual number of edges between the neighbors of the node i, and $k_i(k_i - 1)/2$ denotes the maximum number of edges that could exist between the node i and its neighbors.

The clustering coefficient of the entire network is determined by calculating the average of the clustering coefficients of all nodes, as shown in Eq. (14):

$$V = \frac{\sum_1^N V_i}{N} \tag{14}$$

Robustness assessment metrics

The robustness of an urban metro network indicates its ability to sustain regular operations in the face of unexpected disruptions. In this study, both network efficiency and the relative size of the largest connected subgraph, as proposed by Holme and Kim (2002), are utilized to evaluate network performance following damage.

(1) Network Efficiency (NE).
In an urban metro network, the efficiency between two stations is defined as the inverse of the distance separating them. A shorter distance between stations indicates higher efficiency, which is commonly used to assess the operational efficiency between stations in a metro network. The overall efficiency of an urban metro network is determined by calculating the average of the inverse distances between all pairs of stations. The calculation formula is given in Eq. (15):

$$E = \frac{2}{N(N-1)} \sum\nolimits_{i \neq j} \frac{1}{d_{ij}} \tag{15}$$

where N is the total number of nodes in the network, and d_{ij} represents the distance between node the i and the node j. If the node i and the node j are not connected, $d_{ij} \to \infty$, and hence $\frac{1}{d_{ij}} \to 0$.

(2) Relative size of the largest connected subgraph (RS)
A network may break into several disconnected subnetworks under damage. The subnetwork containing the largest number of nodes is referred to as the largest connected subgraph and is commonly used to assess the network's overall connectivity. The RS is defined as the ratio of its nodes to the total number of nodes in the network after the damage. The formula for this calculation is presented in Eq. (16):

$$R = \frac{N'}{N} \tag{16}$$

where $N\prime$ is the number of nodes in the largest connected subgraph, and N is the total number of nodes in the original network.

Station importance assessment

Current studies often assess node importance using centrality measures such as degree centrality and betweenness centrality. Although degree centrality reflects a node's local connectivity, it overlooks its impact on non-adjacent nodes and the overall network. Betweenness centrality describes a node's influence on the overall network, but it may miss key nodes not located on the shortest paths.

Station importance relates to transportation network efficiency as well as public safety and emergency response. Metro stations face a risk of inundation during extreme weather conditions like heavy rain or flooding. Integrating urban flood vulnerability into station importance assessment allows for a more comprehensive assessment of a station's role and risk within the network. This study incorporates urban flood vulnerability into the composite assessment of station importance, as shown in Eq. (17):

$$F_i = S_i(\lambda C_K(i) + \mu C_B(i)) \tag{17}$$

where F_i represents the composite importance score of the node i,S_i denotes the flood vulnerability score of the node i,$C_K(i)$ is the degree centrality of the node i,$C_B(i)$ is the betweenness centrality of the node i,λ and μ are the weight coefficients assigned to degree centrality and betweenness centrality, and $\lambda + \mu = 1$.

To accurately reflect a station's importance, an optimal set of weight coefficients λ and μ must be selected. This study determines these weight coefficients by experimenting with various values of λ and μ. It assesses station importance and conducts targeted damage on the top 10% of stations based on their importance ranking. By analyzing the changes in NE and RS under each combination of λ and μ, the combination resulting in the greatest variation in E and R is chosen as the optimal set of weight coefficients for assessing station importance.

Cascading failure model

When a node or edge fails, it becomes non-functional. The impact extends beyond the failed node or edge, affecting surrounding components and potentially the entire network. If certain nodes or edges become overloaded, successive failures may occur, potentially leading to partial or complete paralysis of the metro network.

Initial load and maximum capacity

(1) Initial Load

In this study, passenger flow (total entries and exits at a station on a typical workday) is used as the initial load for each node. This approach more accurately represents the operational conditions of the Changsha Metro. Traditional metrics such as degree or betweenness focus mainly on node connectivity and positional importance, but cannot fully capture the actual load on nodes. In contrast, passenger flow reflects the real load distribution of nodes within the subway network, providing a more accurate simulation and analysis of the network's performance during operation. In turn, this offers valuable support for optimizing operational strategies and enhancing passenger experience. The initial load is calculated using Eq. (18):

$$L_i(0) = Q_i \tag{18}$$

where $L_i(0)$ represents the initial load of the node i. Q_i is the total number of passengers entering and exiting the node i on a given workday.

(2) Maximum Capacity

Each station in the urban metro network is assumed to have a certain passenger flow capacity. Based on the model proposed by Motter and Lai (2002), a station's maximum capacity is positively correlated with its initial load and is influenced by a tolerance parameter. The maximum capacity is calculated using Eq. (19):

$$C_i = 1 + \alpha L_i(0) \tag{19}$$

where C_i denotes the maximum capacity of the node i;α is the tolerance parameter($\alpha > 0$).

Load redistribution model

When a node fails or exceeds its capacity, it becomes inoperable which triggers the load redistribution across the network. ΔL_j denotes the load redistributed to each adjacent node after a node failure. Equation (20) defines the load redistribution model:

$$\Delta L_j = \begin{cases} (L_i - C_i) \cdot \frac{C_j - L_j}{\sum_{j \in \phi_i} (C_j - L_j)}, C_i < L_i \leq \gamma C_i \\ L_i \cdot \frac{C_j - L_j}{\sum_{j \in \phi_i} (C_j - L_j)}, L_i > \gamma C_i \\ 0, L_i \leq C_i \end{cases} \tag{20}$$

where ΔL_j is the load increment for the node$j$;γ is the overload capacity adjustment parameter ($\gamma \geq 1$), and ϕ_i is the set of adjacent nodes to the failed node$i$. When the load of the node i is less than its capacity ($L_i \leq C_i$), the node remains in a normal state, and no load is redistributed to its neighboring nodes. When the load exceeds its capacity but is less than its overload capacity ($C_i < L_i \leq \gamma C_i$), the node enters a suspended state, and the load distribution to any of its neighboring nodes is$(L_i - C_i) \cdot \frac{C_j - L_j}{\sum_{j \in \phi_i} (C_j - L_j)}$. When the load exceeds its overload capacity ($L_i > \gamma C_i$), the node fails, and the load distribution to any of its neighboring nodes is $L_i \cdot \frac{C_j - L_j}{\sum_{j \in \phi_i} (C_j - L_j)}$.

Cascading failure propagation process

Based on the load redistribution model, the real-time load of neighboring stations at the time step t is the sum of their previous load and the redistributed load, as shown in Eq. (21):

$$L_j(t) = L_j(t-1)\Delta L_j \tag{21}$$

where $L_j(t)$ represents the real-time load of node j.

The load redistribution necessitates a status reassessment for each node due to affecting the load of neighboring nodes. If a node fails or enters a suspended state, load redistribution continues until the load aligns with the nodes' capacity constraints. If a node reaches a normal state, no further load redistribution occurs. The node state expression is defined by Eq. (22):

$$\Gamma_j(t) = \begin{cases} 0, L_j(t) \le C_j \\ 1, C_j < L_j(t) \le \gamma C_j \\ 2, L_j(t) > \gamma C_j \end{cases} \tag{22}$$

where $\Gamma_j(t)$ denotes the state of node j at time t.$\Gamma_j(t) = 0$ indicates that the node is in a normal state;$\Gamma_j(t) = 1$ indicates that the node is in a suspended state;$\Gamma_j(t) = 2$ indicates that the node is in a failed state.

Cascading failure algorithm and simulation process

Using the cascading failure model for urban metro networks, the simulation process has been systematically organized and is illustrated in the flowchart shown in Fig. 3. This model captures the propagation of failures within the network when disruptions occur, providing a step-by-step framework for analysis. The cascading failure process includes initial failure triggering, load redistribution, and the evaluation of network performance under cascading effects.

Case study

As shown in Fig. 4, the daily average passenger flow in Changsha showed a continuous growth trend, increasing from 6.728 million to 27.784 million from 2018 to 2024, a rise of approximately 3.13 times. This reflects the rapid growth in demand for metro transportation. The Changsha metro network operates six lines. The network spans Changsha's main urban area and Changsha County, with 161 stations, including 19 transfer stations, and an operational length of 236.47 km. This study focuses on the Changsha metro network within the main urban area, excluding the two intercity railways. Specifically, it considers Lines 1 through 6, including 127 stations, as shown in Fig. 5.

(1) The study used operational data from the Changsha metro network up to 2024, covering 127 stations.

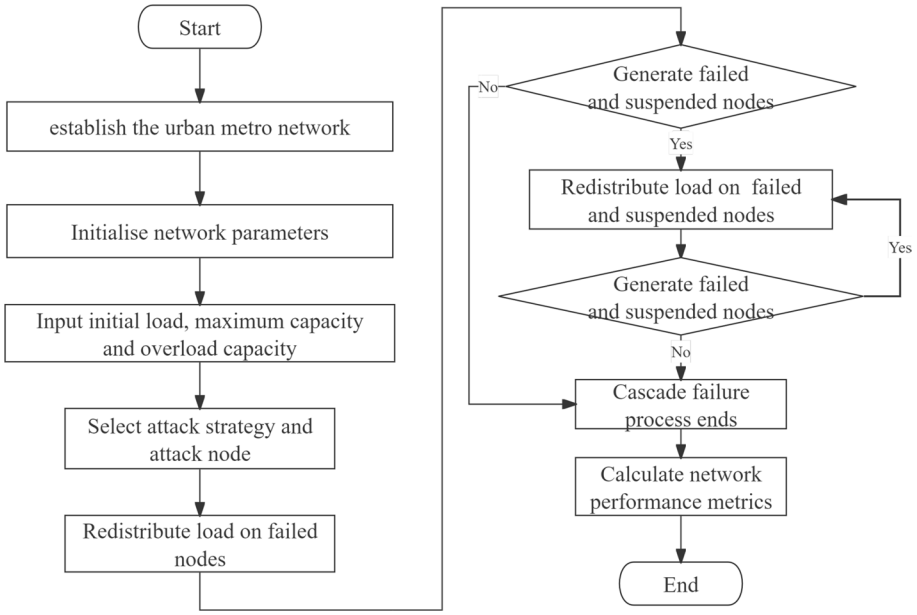

Fig. 3 Cascading failure simulation flow

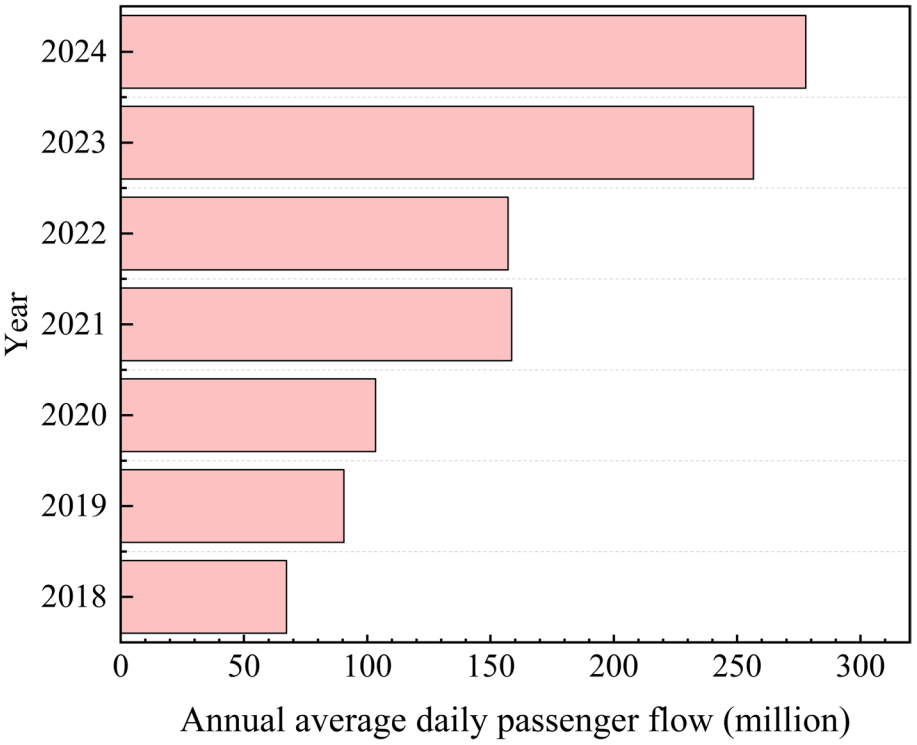

Fig. 4 Changsha metro annual average daily passenger flow

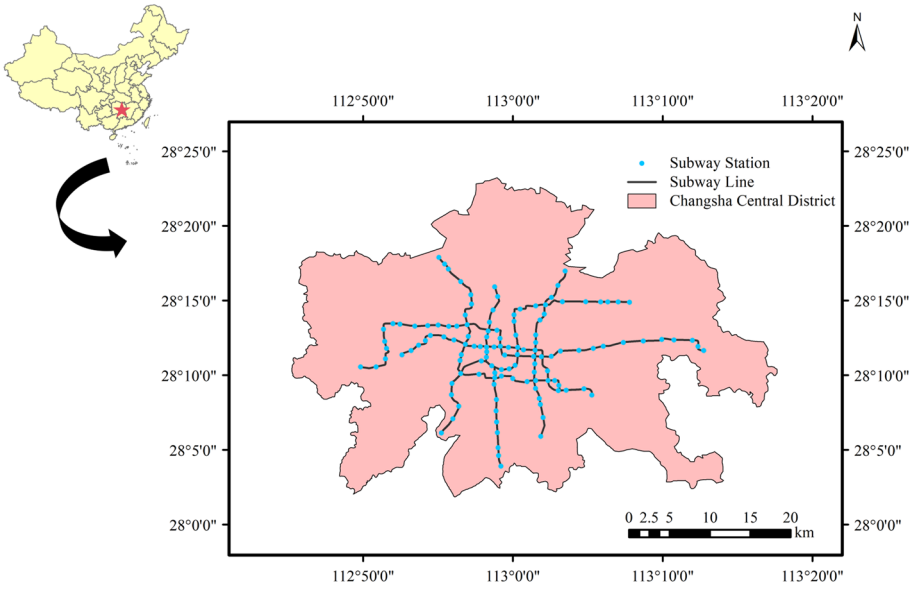

Fig. 5 Topology of Changsha metro network

Table 2 Topological metrics of changsha metro network

Topological metrics	Value
Node	127
Edge	142
Mean of degrees	2.2362
Network efficiency	0.1359
Average shortest path length	11.1976
Clustering coefficient	0.0407

(2) The metro network is modeled as an undirected, unweighted graph, which disregards the travel directions, train schedules, and train categories.

Network characteristics analysis

A 127 × 127 adjacency matrix was constructed to represent the connectivity between stations in the Changsha metro network, with a value of 1 indicating adjacency and 0 otherwise. The adjacency matrix was then imported into Python to compute the topological metrics of the network. The results are summarized in Table 2. The network consists of 127 nodes and 142 edges. And the average shortest path length is 11.1976, indicating that about 11 nodes must be traversed to connect any two nodes. However, the network exhibits low global efficiency, connectivity, and clustering coefficients. Figure 6 illustrates the node degree distribution, where over 70% of the nodes have a degree of 2, and the maximum degree is 4. The average node degree of the network is 2.2362, indicating that each station is, on average, connected to approximately two other stations.

Using the method in Eq. (11), we intentionally damage the top 20 most important stations to investigate the impact of single station failure on network performance. Figure 7 and Fig. 8 show the NE and RS under single station failure. As seen in Table 3, among the top 10 most important stations, the failure of Liugoulong Station and Renmin East Road Station, despite being transfer stations, leads to significant changes in both NE and RS. This is because these two stations serve as the only connection for many other stations, and their failure disconnects parts of the network, drastically reducing NE and RS. The remaining eight stations are transfer points between two metro lines, and while they handle high passenger volumes in operation, their failure can cause cascading effects, increasing the load on adjacent stations and potentially leading to network collapse. Some nodes, despite their high importance ranking, show smaller changes in NE and RS due to dense surrounding connections, where failure does not disrupt connectivity, and alternative paths alleviate congestion.

Analysis of station flood vulnerability

This study utilized various datasets, including topographical information, population data, government fiscal revenue data, Points of Interest (POI) data, and station passenger flow data. The sources of these datasets are provided in Table 7. All data used in this study were collected before 2024, with the passenger flow data representing the number of entries and

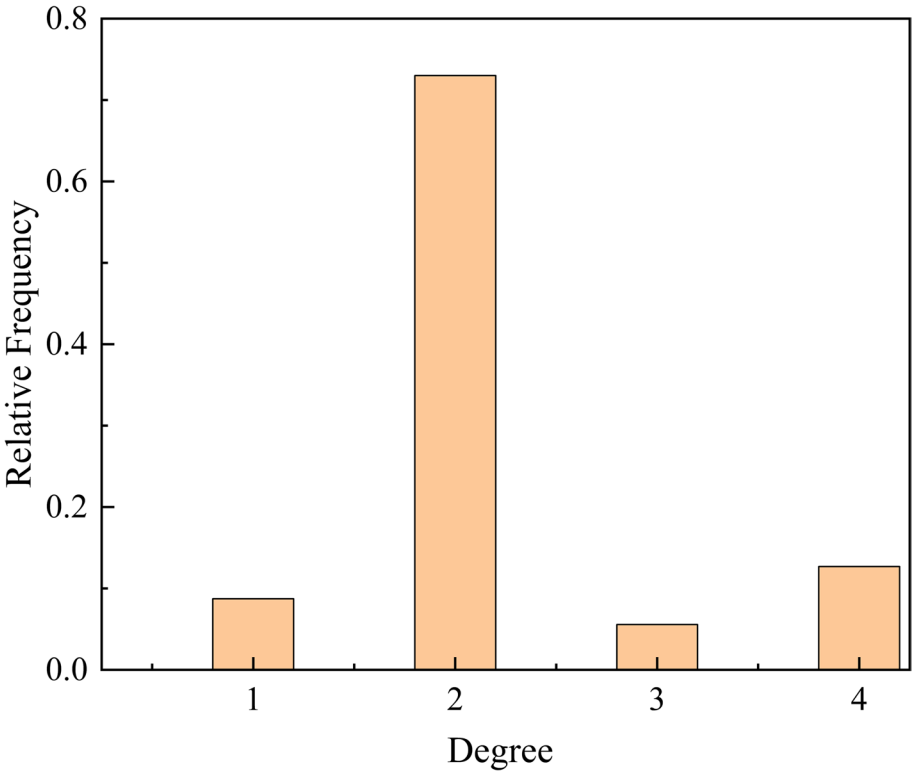

Fig. 6 Changsha metro network degree distribution

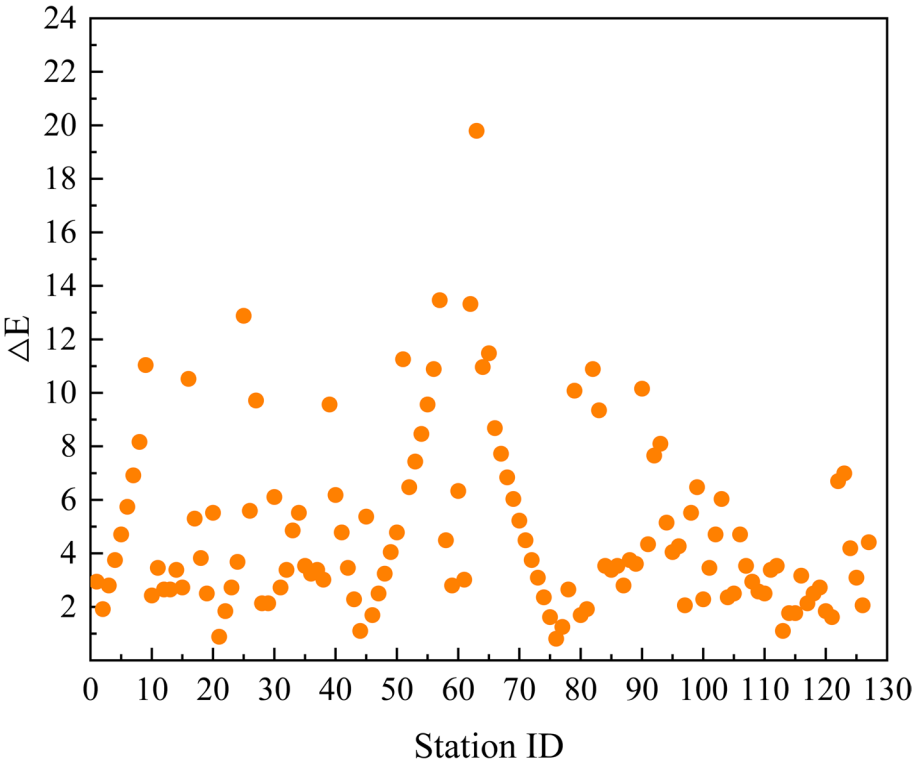

Fig. 7 Rate of change of NE at single station failure

exits at each metro station in Changsha on a typical workday in 2024. Figures 19, 20 and 21 illustrate the spatial distribution of the data.

Based on the comprehensive assessment indicators for station flood vulnerability proposed earlier, the weights of each assessment indicator were calculated using the entropy method. The results are presented in Table 4. Notably, within the sensitivity indicators, the weight values for slope and normalized vegetation coverage, as well as the exposure indicator for station passenger flow, are relatively high. This indicates that these factors significantly influence the flood vulnerability of the stations.

Flood vulnerability at each metro station was assessed using the TOPSIS method for information fusion. The Jenks natural breaks classification (Sujithlal et al. 2024) was then applied to categorize flood vulnerability into four levels: low, medium–low, medium, and high vulnerability. The distribution of flood vulnerability levels across metro stations is shown in Fig. 9. Among the stations, 9 were classified as low vulnerability, 17 as medium–low vulnerability, 28 as medium vulnerability, and 72 as high vulnerability. The data indicate that stations such as Orange Isle, Xiangjiang Middle Road, Wangchengpo, and Changsha Railway Station exhibit high sensitivity to flooding. These stations have previously experienced flooding events that led to service suspensions or station closures. For example, on July 28, 2024, heavy rain caused waterlogging at the entrances, triggering a station closure alarm. Consequently, Wangchengpo Station and Changsha Railway Station were temporarily closed, and Orange Isle Station experienced a temporary service suspension. On June

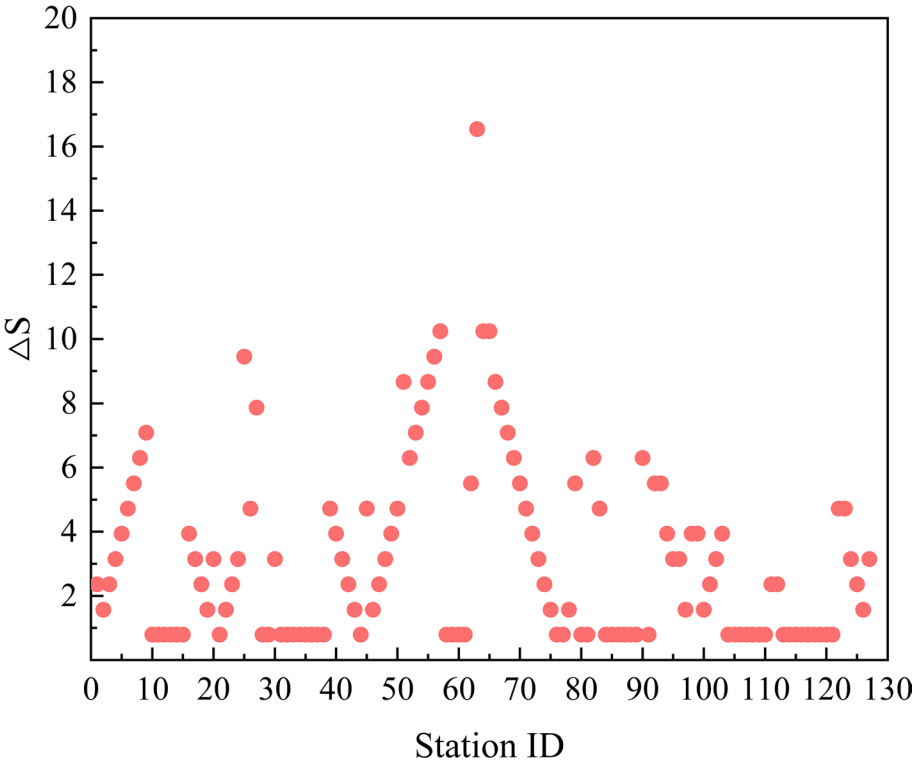

Fig. 8 Rate of change of RS at single station failure

24, 2024, a heavy rainstorm caused severe waterlogging in the plaza of Changsha Railway Station, affecting passengers' access to Exit 6 of the metro station. On July 3, 2017, flooding in Changsha led to the suspension of service at Orange Isle Station and Xiangjiang Middle Road Station.

Stations such as Orange Isle Station and Xiangjiang Middle Road Station are located near the Xiangjiang River and are classified as riverside metro stations. Due to their low elevation and proximity to the river, these stations are highly susceptible to flooding, particularly during heavy rainfall events that lead to a rise in the river's water level. This can result in waterlogging around the metro station entrances. Transportation hubs like Changsha Railway Station and Wangchengpo Station, which experience high passenger volumes, are situated in areas with relatively low vegetation coverage. Additionally, factors such as aging drainage systems can exacerbate the issue. During intense, short-duration rainfall, these stations may struggle to remove waterlogging quickly.

Station importance analysis

Based on the comprehensive assessment indicators for station importance presented earlier, the network performance under various weight combinations is summarized in Table 5. ΔR is the change rate of RS, and ΔE is the change rate of NE. As shown by the bolded data in the table, when the weights are set at $\lambda = 0.9$ and $\mu = 0.1$, the results are as follows: R is

Table 3 Network metric values at single station failure

Order	Station name	R	ΔR	E	ΔE
1	Liugoulong	0.8346	16.5400	0.1090	19.7940
2	Chaoyangcun	0.9921	0.7900	0.1284	5.5188
3	Wenchangge	0.9606	3.9400	0.1216	10.5224
4	Yingbin Road	0.9921	0.7900	0.1273	6.3282
5	Furong District Government	0.9921	0.7900	0.1298	4.4886
6	Renmin East Road	0.8976	10.2400	0.1176	13.4658
7	Shawan Park	0.9370	6.3000	0.1211	10.8904
8	Fubuhe	0.9528	4.7200	0.1229	9.5659
9	Huangtuling	0.9291	7.0900	0.1209	11.0375
10	Yingwanzhen	0.9370	6.3000	0.1221	10.1545
11	Railway Station	0.9921	0.7900	0.1293	4.8565
12	Guitang	0.9528	4.7200	0.1232	9.3451
13	North Yuehu Park	0.9213	7.8700	0.1227	9.7130
14	Wanjiali Square	0.9921	0.7900	0.1295	4.7093
15	South Martyrs Park	0.9921	0.7900	0.1318	3.0169
16	Xiangya Hospital	0.9449	5.5100	0.1178	13.3186
17	Houjiatang	0.9921	0.7900	0.1312	3.4584
18	Wuyi Square	0.9921	0.7900	0.1313	3.3848
19	Dongtang	0.9921	0.7900	0.1313	3.3848
20	The Third Xiangya Hospital	0.8976	10.2400	0.1210	10.9639

Table 4 Flood vulnerability assessment indicators and weighting values

Vulnerability assessment indicators		Weighting values
Sensitivity	Slope	0.1697
	Rainfall	0.1191
	DEM	0.1233
	Normalized difference vegetation index	0.1781
	River density	0.0396
	Road density	0.0396
Exposure	Passenger Flow	0.1776
	Number of entrances and exits	0.0227
	Density of nearby schools	0.0418
	Proportion of vulnerable populations	0.0396
Adaptability	Government fiscal revenue	0.0396
	Density of nearby hospitals	0.0092

0.1826, ΔR is 0.8174, E is 0.0333, and ΔE is 0.1026. The maximum change in network performance occurred with this weight combination. Therefore, this set of weights is chosen as the optimal coefficients for assessing station importance in the Changsha metro network.

Using the formula for calculating station importance in the Changsha metro network and the Jenks natural breaks classification, stations were categorized into four levels: low, moderately low, medium, and high importance. 11 stations were classified as low importance, 60

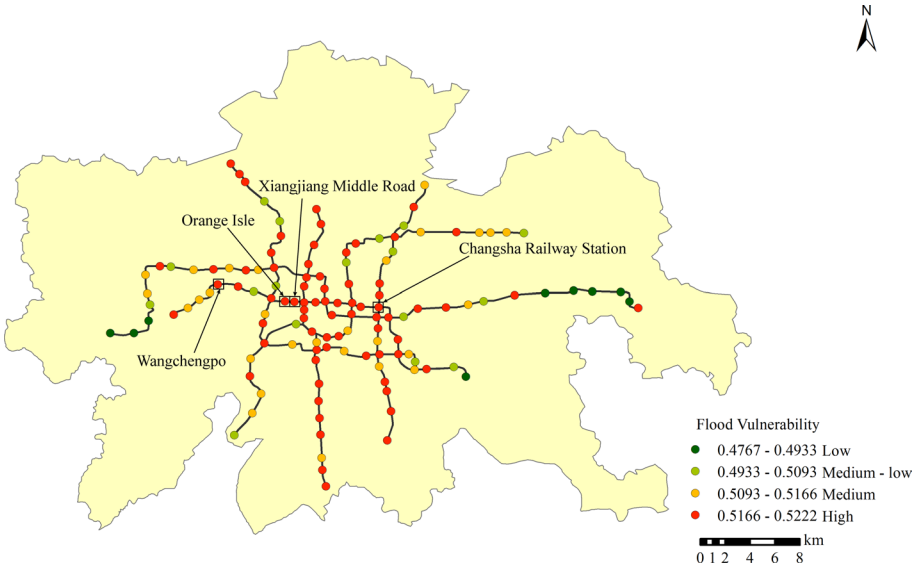

Fig. 9 Distribution of station flood vulnerability

Table 5 Performance of networks with different λ, μ combinations

λ	μ	R	ΔR	E	ΔE
0	1	0.2000	0.8000	0.0417	0.0942
0.1	0.9	0.2000	0.8000	0.0417	0.0942
0.2	0.8	0.2000	0.8000	0.0417	0.0942
0.3	0.7	0.2000	0.8000	0.0417	0.0942
0.4	0.6	0.1826	0.8174	0.0402	0.0957
0.5	0.5	0.1826	0.8174	0.0402	0.0957
0.6	0.4	0.2000	0.8000	0.0372	0.0987
0.7	0.3	0.2000	0.8000	0.0372	0.0987
0.8	0.2	0.2000	0.8000	0.0372	0.0987
0.9	**0.1**	**0.1826**	**0.8174**	**0.0333**	**0.1026**
1	0	0.3739	0.6261	0.0463	0.0896

stations as moderately-low importance, 41 stations as medium importance, and 14 stations as high importance. The distribution of station importance levels is illustrated in Fig. 10. As shown in Fig. 10, stations such as Changsha Railway Station and Liugoulong Station are categorized as high importance. These stations are major transfer hubs with high passenger volume and, in some cases, significant flood vulnerability. Failure of such high-importance stations could result in substantial degradation of the overall metro network performance.

Network robustness analysis

This study utilized targeted damage strategies to assess the robustness of the urban metro network, comparing its robustness under cascading and non-cascading failures. The damage strategies were classified into degree centrality-based damage, vulnerability-based damage,

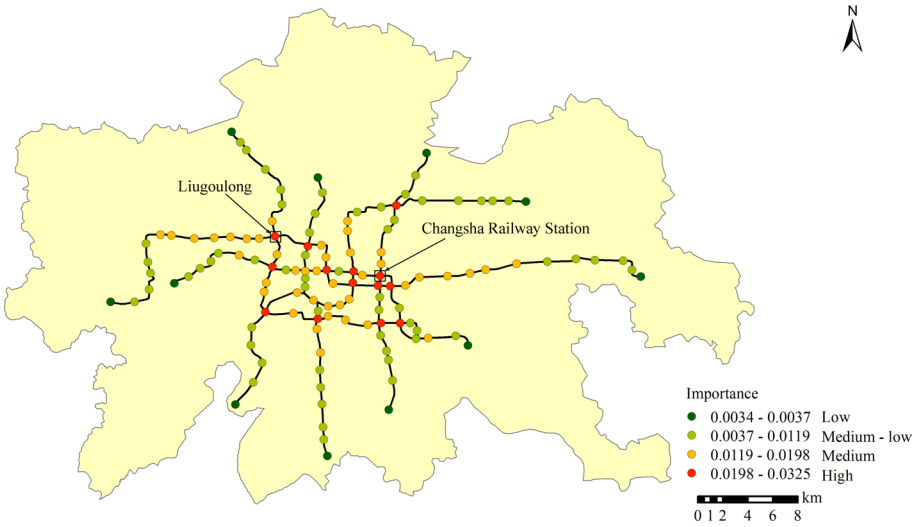

Fig. 10 Distribution of station importance

and importance-based damage. These strategies involve the sequential removal of nodes based on descending orders of node degree centrality, flood vulnerability, and importance values, respectively. Key parameters in the cascading failure model include tolerance and overload capacity adjustment.

Figure 11 illustrates the changes in the RS and NE under various damage strategies, for both cascading and non-cascading failure scenarios. In the non-cascading failure scenario, RS exhibits significant changes under degree centrality-based and importance-based damage, whereas the decline rate is relatively gradual under vulnerability-based damage. This observation aligns with the earlier analysis: degree centrality-based and importance-based damage primarily target nodes that are crucial to the network's structure, while vulnerability-based damage focuses on nodes that are more susceptible to flooding. In non-cascading failures, vulnerability-based damage may not immediately lead to a significant reduction in the RS, as the targeted nodes might not be the most critical components of the network.

In cascading failure scenarios, targeted damage based on degree centrality leads to significant network degradation. Specifically, the removal of nine nodes reduces the RS to 0.1496 and the NE to 0.0131, which corresponds to only 9.64% of the initial efficiency. This substantial decline indicates that these high-degree nodes are indeed critical to maintaining the network's integrity. Similarly, under the targeted damage scenario based on flood vulnerability, the removal of seven nodes leads to a marked deterioration in network performance. Specifically, the NE drops to 0.0065, representing only 4.73% of the initial efficiency, while the RS declines to 0.0866. However, the vulnerability-based attack strategy does not cause significant degradation in the early stages of node removal, suggesting that highly flood-vulnerable nodes may not coincide with topologically critical ones. This indicates a structural–functional mismatch: while upgrading these stations may improve the network's resilience to environmental hazards, it may have a limited impact on enhancing its structural robustness. Therefore, robustness should be addressed through complementary but distinct strategies in metro network planning.

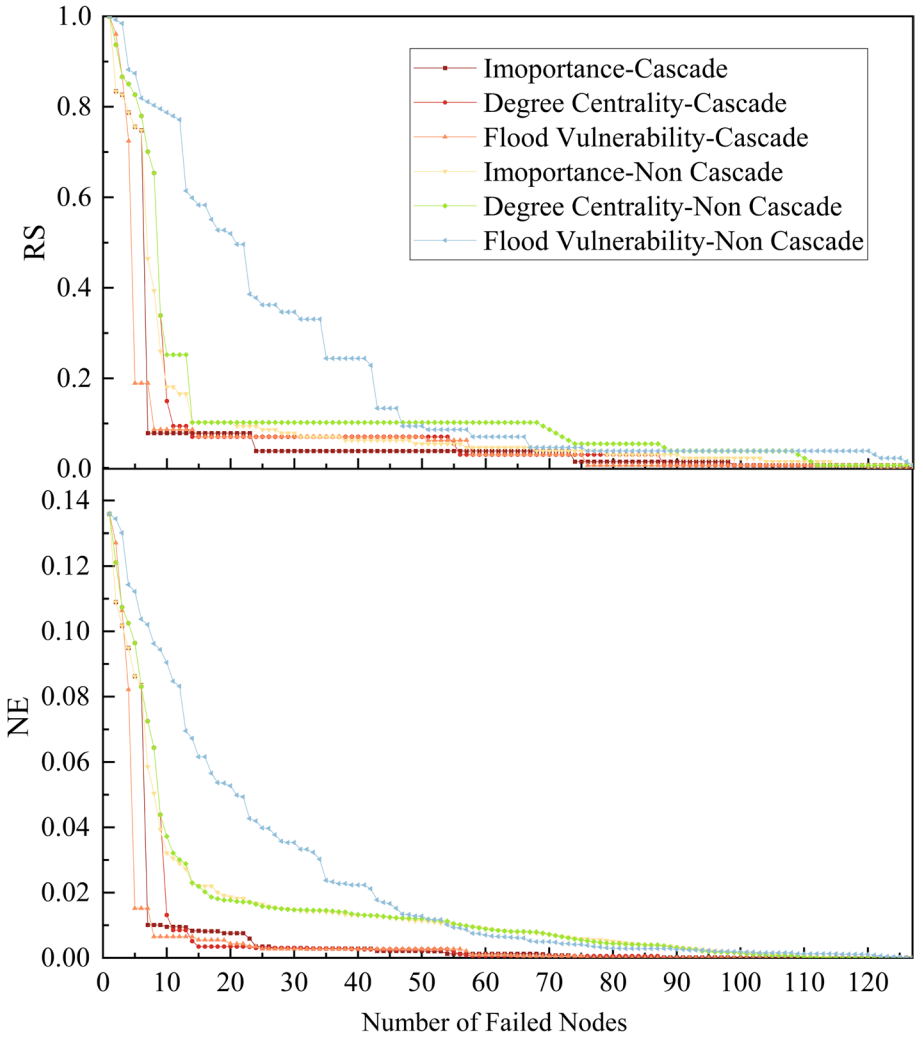

Fig. 11 The RS and NE under different damage strategies

When fewer nodes are removed, damage targeting node importance results in significant impacts due to the propagation of failures. With the removal of six nodes, a comparison across the three targeted attack strategies reveals that the importance-based strategy causes the most severe network degradation, as shown in Table 6. This strategy results in the lowest NE (0.0101) and the smallest RS (0.0787), outperforming degree centrality-based (NE=0.0725, RS=0.7008) and flood vulnerability-based damage (NE=0.0152, RS=0.1890) in terms of disruptive impact.

In relative terms, the importance-based damage reduces NE by 86.07% and 33.55%, and RS by 88.77% and 58.36%, compared to the centrality-based and flood vulnerability-based damage strategies, respectively. These findings indicate that targeted damage based on node importance is markedly more effective in undermining network robustness.

Table 6 The RS and NE after removing the top 6 nodes under different damage strategies

Damage strategies	RS	NE
Importance-based damage	0.0787	0.0101
Degree centrality-based damage	0.7008	0.0725
Vulnerability-based damage	0.1890	0.0152

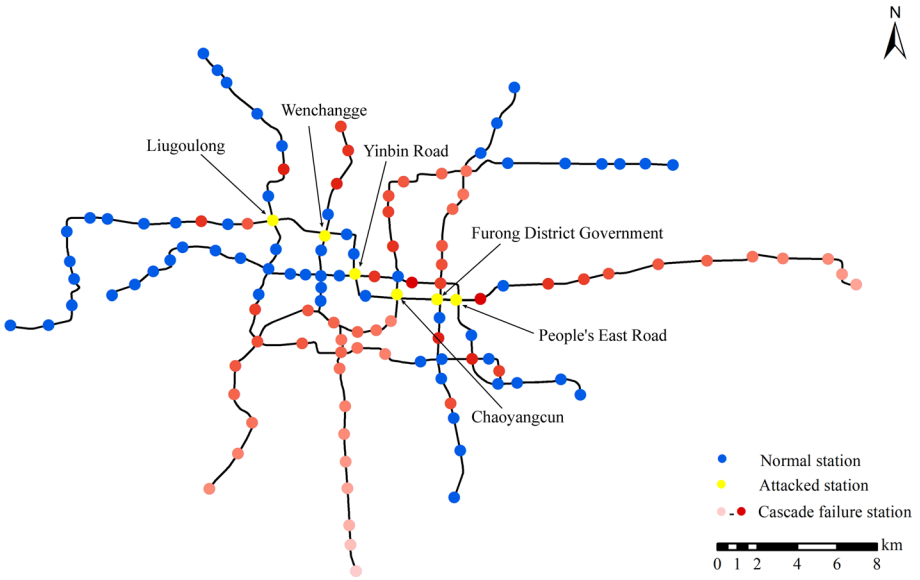

Fig. 12 Cascading failures process for removing the top 6 importance-based stations

The performance trends across different damage strategies exhibit similar patterns in both cascading and non-cascading failure scenarios. Initially, the network's connectivity and efficiency are substantially impacted, leading to a rapid decrease in the RS and NE. In the later stages, the changes diminish, and the overall trend stabilizes.

In Fig. 12, red nodes indicate those that have failed due to the initial damage, with darker colors representing nodes that failed earlier in the sequence. When the top six stations—Liugoulong Station, Chaoyangcun Station, Wenchangge Station, Yingbin Road Station, Furong District Government Station, and People's East Road Station—are simultaneously damaged and fail, neighboring stations are the first to be affected by cascading failures. Due to the high significance of these stations, their failure triggers cascading impacts on other stations.

Figures 13 and 14 further demonstrate that the removal of high-importance nodes triggers multiple rounds of load redistribution under cascading failure conditions, resulting in extensive station failures and widespread network paralysis.

Both the tolerance parameter α and the overload adjustment parameter γ influence the robustness of the network under cascading failures. Based on the parameter settings proposed by Xing et al. (2018), α and γ are varied within a referenced range to simulate failure propagation. Figures 15 and 16 demonstrate how varying α (with an overload adjustment parameter γ=1.5) affects the network when nodes are removed. When up to five nodes are removed, variations in α do not significantly affect the RS. The values and trends of the RS remain consistent across varying α values. However, when more than five nodes fail,

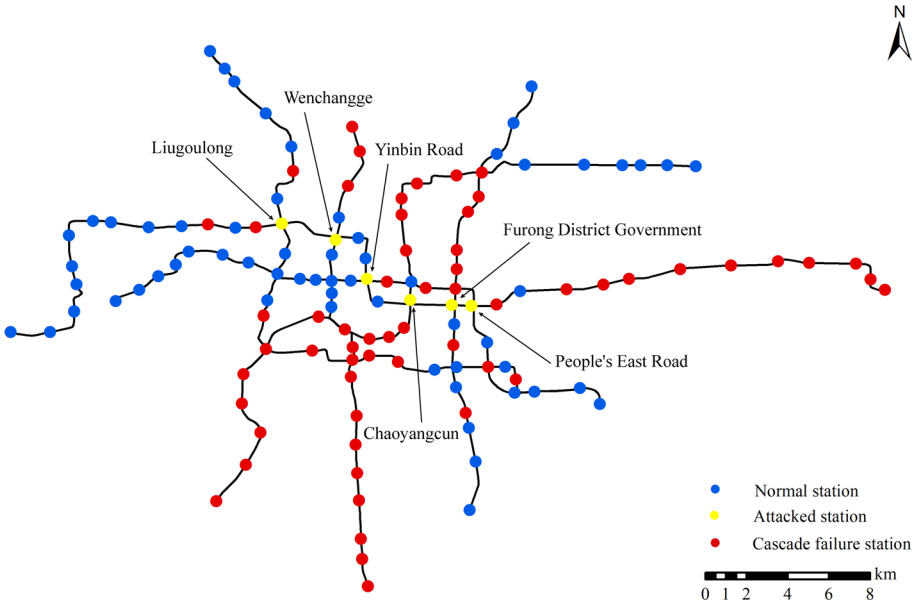

Fig. 13 Cascading failures result after removing the top 6 importance-based stations

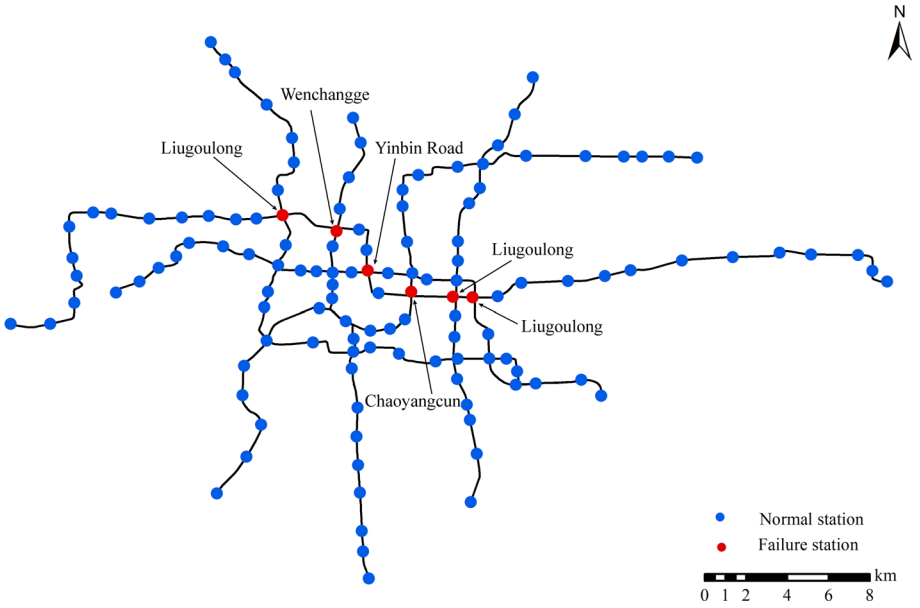

Fig. 14 Non-cascading failure result after removing the top 6 importance-based stations

increasing α mitigates the decline in both the RS and NE. This occurs because increasing the maximum capacity of nodes reduces the likelihood of cascading failures and their impact on the network. Thus, enhancing the capacity of critical stations during urban metro network expansion can mitigate the effects of cascading failures, improve network robustness, and ensure safe and reliable urban metro operations.

The overload adjustment parameter γ affects network robustness during cascading failures. Figures 17 and 18 demonstrate the impact of varying γ (with a tolerance parameter α = 0.25) on the Changsha Metro network during cascading failures.

When the number of damaged nodes remains below five, increasing the overload adjustment parameter γ gradually raises both the RS and NE for a given number of failed nodes. However, in later stages, the influence of varying overload adjustment parameters γ on the network diminishes. This suggests that while increasing γ initially enhances the network's capacity to handle failures, its impact becomes less pronounced as more nodes fail.

The analysis reveals that the Changsha metro network is significantly more vulnerable when cascading failures are considered. Regardless of cascading failure, targeted damage initially exhibits a similar decreasing trend. In the case of cascading failures, a sudden and widespread network collapse occurs after a certain number of nodes fail. Conversely, in the absence of cascading failures, the network's performance tends to stabilize over time. Both scenarios demonstrate significant vulnerability to targeted damage.

To enhance the overall robustness of urban metro networks, it is essential to adopt a coordinated governance approach that integrates both structural importance and environmental vulnerability of stations. Structurally critical stations should be prioritized for robustness

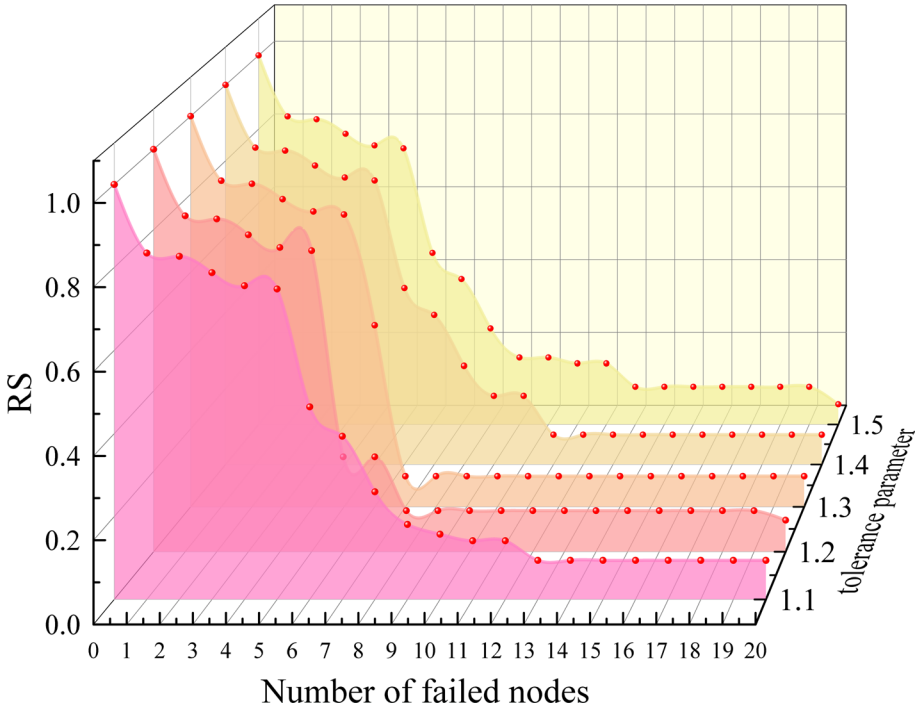

Fig. 15 The RS with different tolerance parameters

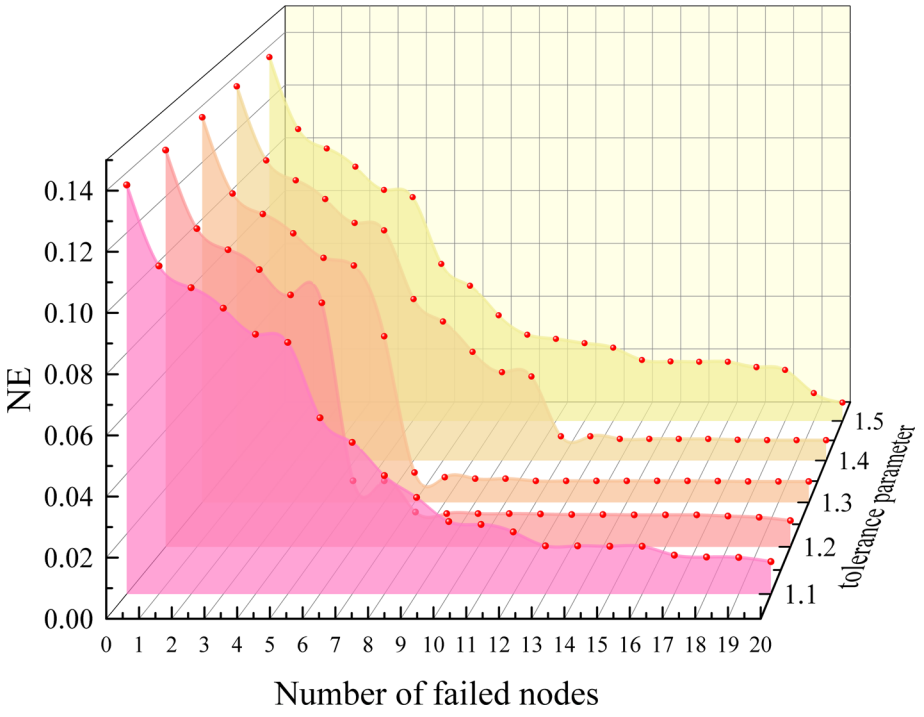

Fig. 16 The NE with different tolerance parameters

enhancements, such as capacity expansion and route optimization. Meanwhile, stations that are not topologically central but highly vulnerable to flooding should receive targeted interventions, including improved drainage, waterproofing measures, and early warning systems. By aligning infrastructure investment with both network criticality and environmental risk, planners can develop more targeted and cost-effective adaptation strategies. This approach helps balance robustness and disaster resilience in metro system planning and flood risk management, contributing to more comprehensive and efficient system performance.

Conclusion

This study assessed the impact of flooding on the urban metro network in Changsha, China, by integrating a cascading failure model. The main conclusions are as follows:

(1) The analysis reveals that network vulnerability increases under cascading failures. The cascading failure model, which incorporates flooding vulnerability along with topological metrics, provides a more accurate representation of metro network conditions.
(2) The network is most vulnerable to damage targeting critical stations. Removing the six most important nodes out of 127 causes the RS to drop sharply to 0.0787, while the NE declines to 0.01, representing 7.36% of the initial efficiency. This highlights the vital role of these nodes in ensuring the stability of the network.

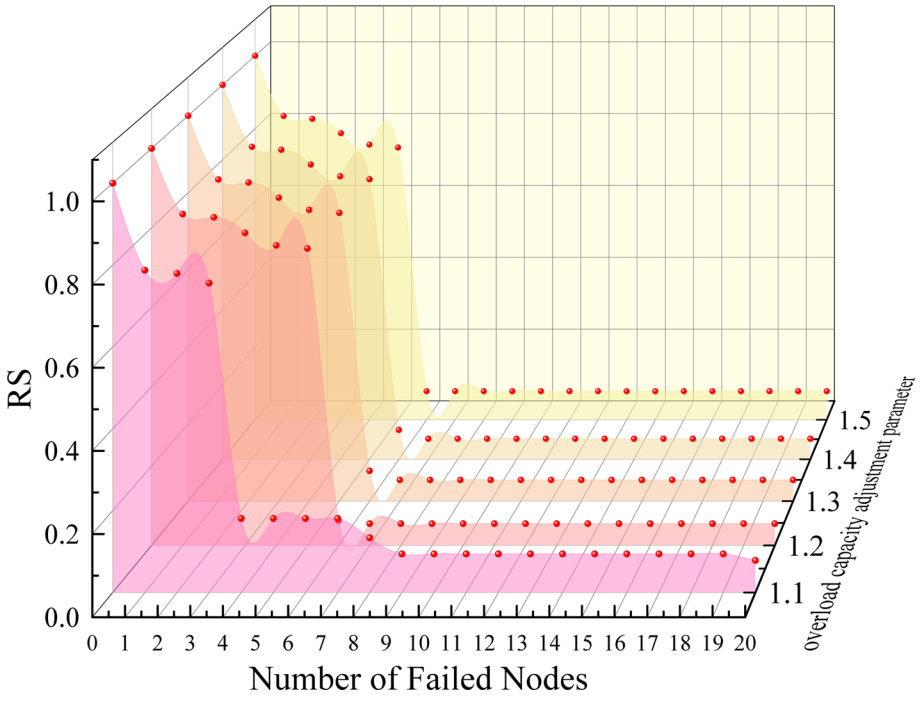

Fig. 17 The RS with different overload capacity adjustment parameters

(3) The residual capacity coefficient and overload adjustment parameter impact network robustness under cascading failures. Although their influence is limited, increasing these parameters within a certain range can reduce cascading failures and mitigate performance declines. For urban metro station reconstruction and expansion, it is recommended to increase capacity beyond daily passenger demand to enhance residual capacity.

This study introduced a method that combines the entropy method and TOPSIS to quantify the flood vulnerability of metro stations, integrating network topology to assess station importance. A cascading failure model was applied to assess the robustness of the metro network under damage scenarios, employing metrics such as NE and RS. Future research could utilize high-precision hydrodynamic models to simulate water accumulation at metro station entrances under different rainfall intensities. This facilitates a comprehensive and accurate analysis of the impact of flooding on metro network performance. Additionally, integrating the metro network with bus, road, and other transport networks should be considered to develop a multi-modal transportation network for resilience studies. This integration would provide valuable insights for the daily maintenance and disaster prevention of urban transportation systems.

The evaluation of network robustness is currently based solely on topological indicators—NE and RS. These metrics, although widely used, primarily reflect structural characteristics and may not fully capture the functional performance of the metro system under disruption. Future research could incorporate functional indicators such as passenger flow

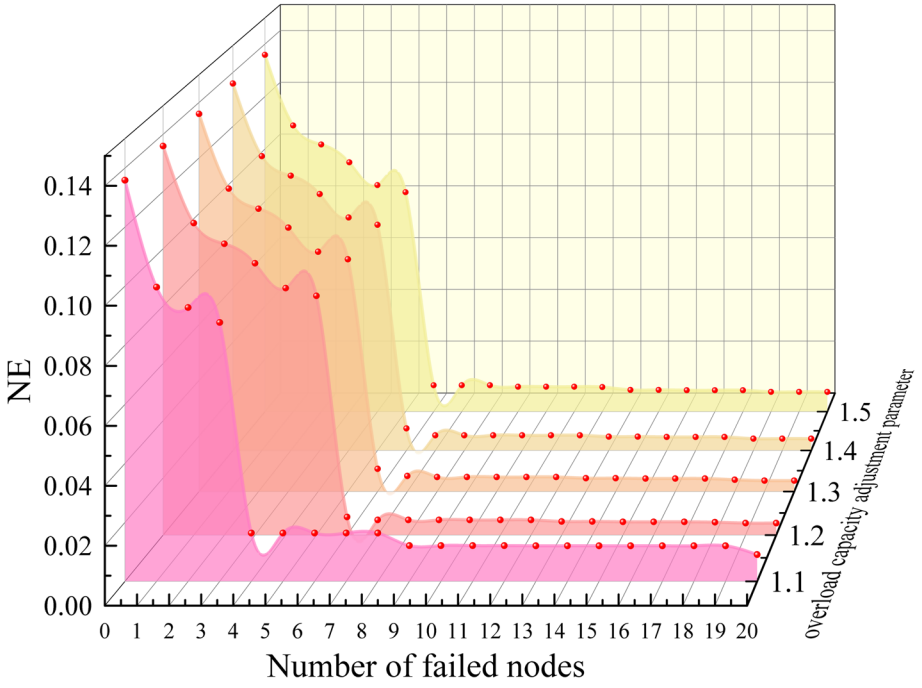

Fig. 18 The NE with different overload capacity adjustment parameters

distribution, travel demand shifts, or accessibility measures to offer a more comprehensive understanding of system resilience. In addition, if sufficient hydrological and infrastructure data become available, future studies could integrate hydrodynamic modeling to simulate the internal flooding processes of metro stations under extreme rainfall scenarios. This would enable a more accurate and detailed assessment of station-level risk and network-wide impact under flood conditions. In future research, the restoration sequence of affected metro stations could be optimized by jointly considering their flood vulnerability and overall importance within the network. Incorporating such post-flood recovery strategies would provide valuable insights for improving the efficiency and effectiveness of urban metro network resilience planning.

Appendix 1

See Table 7.

Table 7 Types and sources of data for the study

Parameters	Data types	Source
Passenger flow	Attribute data	Changsha Metro Group Co.,ltd
Number of entrances and exits	Attribute data	https://www.amap.com/
Density of nearby schools	POI	https://www.amap.com/
Proportion of vulnerable populations	Attribute data	Changsha statistical yearbook
Rainfall	Raster data	https://data.tpdc.ac.cn
DEM	Raster data	https://www.nasa.gov
Slope	Raster data	https://www.nasa.gov
Normalized difference vegetation Index	Raster data	https://www.nasa.gov
River density	Attribute data	https://www.openstreetmap.org
Road density	Attribute data	https://www.openstreetmap.org
Government fiscal revenue	Attribute data	Changsha statistical yearbook
Density of nearby hospitals	POI	https://www.amap.com/

Appendix2

See Figs. 19, 20 and 21.

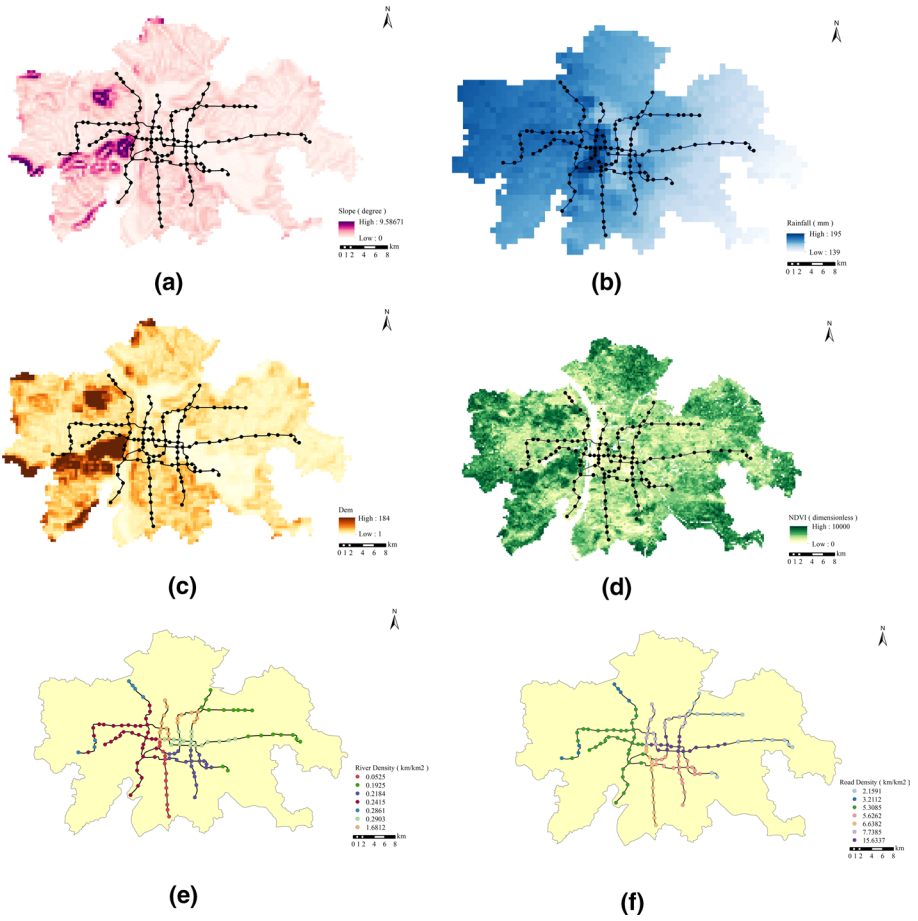

Fig. 19 Spatial distribution of sensitivity indicators

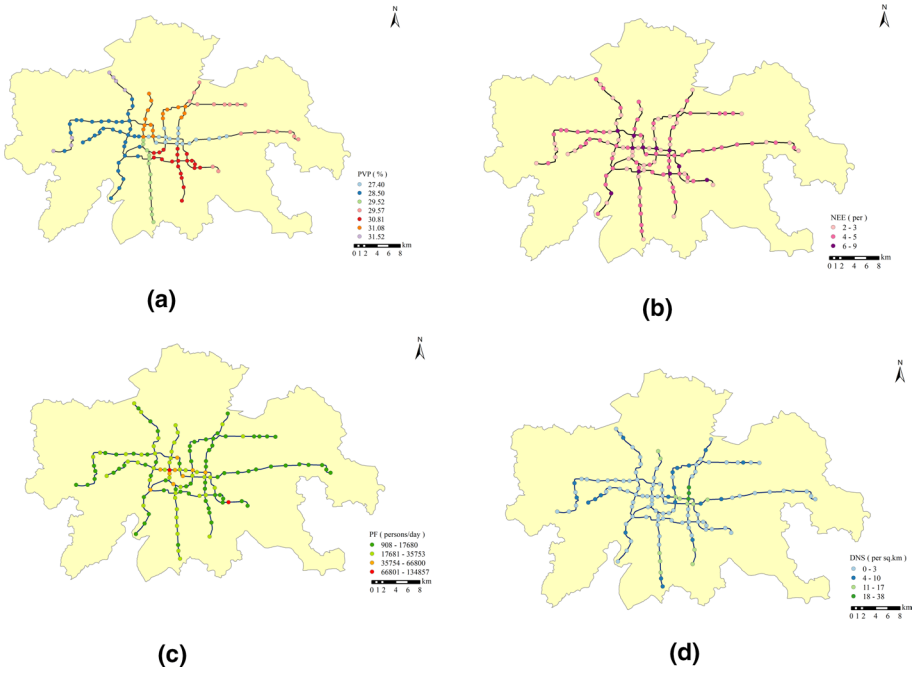

Fig. 20 Spatial distribution of exposure indicators

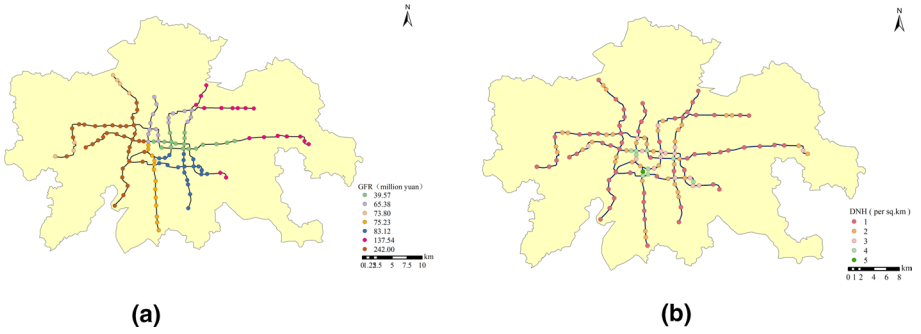

Fig. 21 Spatial distribution of adaptability indicators

Author contribution L.J. and L.Y. wrote the main manuscript text, O.J.H. performed partial data processing, and Z.S.H., L.C.R., and Z.Y. provided funding support. All authors reviewed the manuscript.

Funding Department of Science and Technology of Hunan Province(2022SK2096);Department of Science and Technology of Hunan Province,2022SK2096,The science and technology Program of Hunan Provincial Department of Transportation,202203,202322,The Key Laboratory of Geological Safety of Coastal Urban Underground Space,BHKF2023Y04,The Natural Science Foundation of Changsha,kq2402072,China-Norway Partnership in Smart Sustainable Metropolitan Transport,UTF-2020/10115,the National Natural Science Foundation of China,No.52278306,the HunanProvincial Natural Science Foundation of China,No.2023JJ70003

Data availability No datasets were generated or analysed during the current study.

Conflict of interests The authors declare no conflict of interests.

References

Cabrera, J.S., Lee, H.S.: Flood risk assessment for Davao Oriental in the Philippines using geographic information system-based multi-criteria analysis and the maximum entropy model. J. Flood Risk Manag. **13**(No.2), e12607 (2020). https://doi.org/10.1111/jfr3.12607

Chen, P., Zhang, J., Zhang, L., Sun, Y.: Evaluation of resident evacuations in urban rainstorm waterlogging disasters based on scenario simulation: Daoli District (Harbin, China) as an example. Int. J. Environ. Res. Public Health **11**(No.10), 9964–9980 (2014). https://doi.org/10.3390/ijerph111009964

Chen, Y., Wang, D., Zhang, L., Guo, H., Ma, J., Gao, W.: Flood risk assessment of Wuhan, China, using a multi-criteria analysis model with the improved AHP-entropy method. Environ. Sci. Pollut. Res. Int. **30**(No.42), 96001–96018 (2023). https://doi.org/10.1007/s11356-023-29066-8

Chen, Z., Zheng, C., Tao, T., Wang, Y.: Reliability analysis of urban road traffic network under targeted attack strategies considering traffic congestion diffusion. Reliab. Eng. Syst. Saf. **248**, 110171 (2024). https://doi.org/10.1016/j.ress.2024.110171

China, M. o. T. o. t. P. s. R. o. (2024). *Quick Facts on Urban Rail Transit Operations Data for October 2024*. https://www.camet.org.cn/xytj/tjxx/

Diriba, D., Takele, T., Karuppannan, S., Husein, M.: Flood hazard analysis and risk assessment using remote sensing, GIS, and AHP techniques: a case study of the Gidabo Watershed, main Ethiopian Rift, Ethiopia. Geomatics Nat. Hazards Risk **15**(No.1), 2361813 (2024). https://doi.org/10.1080/19475705.2024.2361813

Dong, S., Wang, H., Mostafavi, A., Gao, J.: Robust component: A robustness measure that incorporates access to critical facilities under disruptions(Article). J. Royal Soc. Interface (2019). https://doi.org/10.1098/rsif.2019.0149

Duan, C., Zhang, J., Chen, Y., Lang, Q., Zhang, Y., Wu, C., Zhang, Z.: Comprehensive risk assessment of urban waterlogging disaster based on MCDA-GIS integration: the case study of Changchun, China. Remote Sens. **14**(No.13), 3101 (2022). https://doi.org/10.3390/rs14133101

Frutos Bernal, E., Mart, Iacute, & n del Rey, A.: Study of the structural and robustness characteristics of madrid metro network. Sustainability, 11(12), 3486 (2019) https://doi.org/10.3390/su11123486

Guan, X., Yu, F., Xu, H., Li, C., Guan, Y.: Flood risk assessment of urban metro system using random forest algorithm and triangular fuzzy number based analytical hierarchy process approach. Sustain. Cities Soc. **109**, 105546 (2024). https://doi.org/10.1016/j.scs.2024.105546

Hallegatte, S., Green, C., Nicholls, R.J., Corfee-Morlot, J.: Future flood losses in major coastal cities. Nat. Clim. Change **3**(No.9), 802–806 (2013). https://doi.org/10.1038/nclimate1979

Hamidi, A.R., Wang, J., Guo, S., Zeng, Z.: Flood vulnerability assessment using MOVE framework: a case study of the northern part of district Peshawar, Pakistan(Article). Nat. Haz. (2020). https://doi.org/10.1007/s11069-020-03878-0

Hieu, T.V., Ann, C.S., Dung, B.N.: Complex network analysis of the robustness of the hanoi, Vietnam Bus Network. J. Syst. Sci. Complexity **32**(5), 1251–1263 (2019)

Holme, P., Kim, B.J.: Attack vulnerability of complex networks. Phys. Rev. E Stat. Nonlinear Soft Matter Phys. **65**(No.5Part2), 056109 (2002). https://doi.org/10.1103/PhysRevE.65.056109

Hoque, M.A.-A., Tasfia, S., Ahmed, N., Pradhan, B.: Assessing spatial flood vulnerability at Kalapara Upazila in Bangladesh using an analytic hierarchy process. Sensors **19**(No.6), 1302 (2019). https://doi.org/10.3390/s19061302

Huang, W., Zhou, B., Yu, Y., Sun, H., Xu, P.: Using the disaster spreading theory to analyze the cascading failure of urban rail transit network. Reliab. Eng. Syst. Saf. **215**(Suppl C), 107825 (2021). https://doi.org/10.1016/j.ress.2021.107825

Huang, W., Li, H., Yin, Y., Zhang, Z., Xie, A., Zhang, Y., Cheng, G.: Node importance identification of unweighted urban rail transit network: an adjacency information entropy based approach. Reliab. Eng. Syst. Saf. **242**, 109766 (2024). https://doi.org/10.1016/j.ress.2023.109766

Khazeiynasab, S.R., Qi, J.: Resilience analysis and cascading failure modeling of power systems under extreme temperatures. J. Modern Power Syst. Clean Energy **9**(6), 1446–1457 (2021)

Li, Z., Tang, X., Li, L., Chu, Y., Wang, X., Yang, D.: GIS-based risk assessment of flood disaster in the Lijiang River Basin. Sci. Rep. (2023). https://doi.org/10.1038/s41598-023-32829-5

Li, D., Hou, Y., Du, S., Zhou, F.: Cascading failure and resilience of urban rail transit stations under flood conditions: a case study of Shanghai Metro. Water **16**(No.19), 2731 (2024). https://doi.org/10.3390/w16192731

Lin, D., Nelson, J.D., Beecroft, M., Cui, J.: Understanding China's metro development: a comparative regional analysis. Res. Transp. Bus. Manag. **47**, 100940 (2022a). https://doi.org/10.1016/j.rtbm.2022.100940

Lin, H., Xia, Y.-X., Jiang, L.-R.: Routing in spatial networks based on shortest path length. Acta Phys. Sin. (2022b). https://doi.org/10.7498/aps.71.20211621

Liu, Y., Yang, J., Geng, P.: Cascading failure of complex networks under degree-based attack. Int. J. Biometrics **13**(No.4), 464–478 (2021). https://doi.org/10.1504/ijbm.2021.117845

Lu, Q.-C., Zhang, L., Xu, P.-C., Cui, X., Li, J.: Modeling network vulnerability of urban rail transit under cascading failures: a coupled map lattices approach. Reliab. Eng. Syst. Saf. **221**, 108320 (2022). https://doi.org/10.1016/j.ress.2022.108320

Lyu, H., Sun, W., Shen, S., Arulrajah, A.: Flood risk assessment in metro systems of mega-cities using a GIS-based modeling approach. Sci. Total. Environ. (2018). https://doi.org/10.1016/j.scitotenv.2018.01.138

Lyu, H.-M., Shen, S.-L., Zhou, A., Zhou, W.-H.: Data in flood risk assessment of metro systems in a subsiding environment using the interval FAHP-FCA approach. Data Brief **26**, 104468 (2019). https://doi.org/10.1016/j.dib.2019.104468

Ma, F., Liang, Y., Yuen, K.F., Sun, Q., Zhu, Y., Wang, Y., Shi, W.: Assessing the vulnerability of urban rail transit network under heavy air pollution: a dynamic vehicle restriction perspective. Sustain. Cities Soc. **52**, 101851 (2020). https://doi.org/10.1016/j.scs.2019.101851

Ma, S., Lyu, S., Zhang, Y.: Weighted clustering-based risk assessment on urban rainstorm and flood disaster. Urban Clim. **39**(Suppl C), 100974 (2021). https://doi.org/10.1016/j.uclim.2021.100974

Ma, Z., Liu, J., Chien, S.I.-J., Hu, X., Shao, Y.: Identifying critical stations affecting vulnerability of a metro network considering passenger flow and cascading failure: case of Xi'an metro in China. ASCE-ASME J. Risk Uncertain. Eng. Syst. Part A Civ. Eng. **9**(No.2), 04023014 (2023). https://doi.org/10.1061/ajrua6.Rueng-1013

Mahmoodi, E., Azari, M., Dastorani, M.T.: Comparison of different objective weighting methods in a multi-criteria model for watershed prioritization for flood risk assessment using morphometric analysis. J. Flood Risk Manag. **16**(No.2), e12894 (2023). https://doi.org/10.1111/jfr3.12894

Majumdar, B.B., Dissanayake, D., Rajput, A.S.: Prioritizing metro service quality attributes to enhance commuter experience: TOPSIS ranking and importance satisfaction analysis methods. Transp. Res. Rec. **2674**(No.6), 124–139 (2020). https://doi.org/10.1177/0361198120917972

Motter, A.E., Lai, Y.-C.: Cascade-based attacks on complex networks. Phys. Rev. E Stat. Nonlinear Soft Matter Phys. **66**(No.6Part2), 065102 (2002). https://doi.org/10.1103/PhysRevE.66.065102

Mouronte-Lopez, M.L.: Analysing the vulnerability of public transport networks. J. Adv. Transp. (2021). https://doi.org/10.1155/2021/5513311

Mussone, L., Salgado, V.J.A., Notari, R.: Evaluation of robustness in underground networks. Phys. A Stat. Mech. Appl. **651**, 130014 (2024). https://doi.org/10.1016/j.physa.2024.130014

Pei, Y., Xie, F., Wang, Z., Dong, C.: Resilience measurement of bus-subway network based on generalized cost. Mathematics **12**(No.14), 2191 (2024). https://doi.org/10.3390/math12142191

Pu, C., Yang, F., Wang, X.: Flood risk assessment of slums in Dhaka city. Geocarto Int. **39**(No.1), 2341802 (2024). https://doi.org/10.1080/10106049.2024.2341802

Qi, Q., Meng, Y., Zhao, X., Liu, J.: Resilience assessment of an urban metro complex network: a case study of the Zhengzhou Metro. Sustainability **14**(11555), 11555 (2022). https://doi.org/10.3390/su141811555

Rafiul Alam, Z.Q., Moulds, S., Radia, M.A., Sara, H.H., Hasan, M.T., Butler, A.: Dhaka city water logging hazards: area identification and vulnerability assessment through GIS-remote sensing techniques. Environ. Monitoring Assess. (2023). https://doi.org/10.1007/s10661-023-11106-y

Roopnarine, C., Ramlal, B., Roopnarine, R.: A comparative analysis of weighting methods in geospatial flood risk assessment: a Trinidad case study. Land **11**(10), 1649 (2022). https://doi.org/10.3390/land11101649

Roy, S., Bose, A., Chowdhury, I.R.: Flood risk assessment using geospatial data and multi-criteria decision approach: a study from historically active flood-prone region of Himalayan foothill, India. Arabian J. Geosci. (2021). https://doi.org/10.1007/s12517-021-07324-8

Sahu, A.S.: A study on moyna basin water-logged areas (india) using remote sensing and GIS methods and their contemporary economic significance. Geography J. (2014). https://doi.org/10.1155/2014/401324

Sar, N., Chatterjee, S., Das Adhikari, M.: Integrated remote sensing and GIS based spatial modelling through analytical hierarchy process (AHP) for water logging hazard, vulnerability and risk assessment in Keleghai river basin, India. Model. Earth Syst. Environ. (2015). https://doi.org/10.1007/s40808-015-0039-9

Shen, Y., Yang, H., Ren, G., Ran, B.: Model cascading overload failure and dynamic vulnerability analysis of facility network of metro station. Reliab. Eng. Syst. Saf. **242**(Suppl C), 109711 (2024). https://doi.org/10.1016/j.ress.2023.109711

Sujithlal, S.P., Ahana, K.K., Satheesan, K., Kottayil, A.: Identification of the tropopause using the Jenks natural breaks classification from 205-MHz stratosphere-troposphere wind profiler radar. IEEE Trans. Geosci. Remote Sens. **62**, 1–6 (2024). https://doi.org/10.1109/tgrs.2024.3386564

Tayyab, M.: Gis-based urban flood resilience assessment using urban flood resilience model: a case study of Peshawar City, Khyber Pakhtunkhwa, Pakistan. Remote Sens. **13**(10), 1864 (2021). https://doi.org/10.3390/rs13101864

Turner, B.L., Kasperson, R.E., Matsone, P.A., McCarthy, J.J., Corell, R.W., Christensene, L., Eckley, N., Kasperson, J.X., Luers, A., Martello, M.L., Polsky, C., Pulsipher, A., Schiller, A.: A framework for vulnerability analysis in sustainability science. Proc. Natl. Acad. Sci. United States America (2003). https://doi.org/10.1073/pnas.1231335100

Wang, Y., Tian, C.: Measure vulnerability of metro network under cascading failure. IEEE Access **9**, 683–692 (2021). https://doi.org/10.1109/access.2020.3046011

Wang, W.-J., Kim, D., Kim, G., Kim, K.T., Kim, S., Kim, H.S.: Flood risk assessment of the Naeseongcheon stream basin, Korea using the grid-based flood risk index. J. Hydrol. Reg. Stud. **51**, 101619 (2024a). https://doi.org/10.1016/j.ejrh.2023.101619

Wang, Y., Zhang, Q., Lin, K., Liu, Z., Liang, Y.-S., Liu, Y., Li, C.: A novel framework for urban flood risk assessment: multiple perspectives and causal analysis. Water Res. **256**, 121591 (2024b). https://doi.org/10.1016/j.watres.2024.121591

Wu, M., Wu, Z., Ge, W., Wang, H., Shen, Y., Jiang, M.: Identification of sensitivity indicators of urban rainstorm flood disasters: a case study in China. J. Hydrol. **599**(Suppl C), 126393 (2021). https://doi.org/10.1016/j.jhydrol.2021.126393

Xing, R., Yang, Q., Zheng, L.: Research on cascading failure model of urban regional traffic network under random attacks. Discrete Dyn Nat Soc (2018). https://doi.org/10.1155/2018/1915695

Xu, J., Song, S., Zhai, H., Yuan, P., Chen, M.: A new analytical framework for network vulnerability on subway system. Concurrency Comput. Pract. Exp. **32**(No.23), e5508 (2019). https://doi.org/10.1002/cpe.5508

Yang, Y., Liu, Y., Zhou, M., Li, F., Sun, C.: Robustness assessment of urban rail transit based on complex network theory: a case study of the Beijing Subway. Safety Sci (2015). https://doi.org/10.1016/j.ssci.2015.06.006

Yang, L., Ni, G., Tian, F., Niyogi, D.: Urbanization exacerbated rainfall over European suburbs under a warming climate. Geophys. Res. Lett. **48**(No.21), e2021GL095987 (2021). https://doi.org/10.1029/2021gl095987

Yang, J., Zhu, D., Zhao, R.: Evaluation of station importance and cascading failure resistance analysis of urban rail transit network. China Safety Sci. J. **32**(8), 161–167 (2022)

Yin, X., Wu, J.: Research on the performance recovery strategy model of Hangzhou Metro Network based on complex network and tenacity theory. Sustainability **15**, 6613 (2023). https://doi.org/10.3390/su15086613

Yin, D., Huang, W., Shuai, B., Liu, H., Zhang, Y.: Structural characteristics analysis and cascading failure impact analysis of urban rail transit network: From the perspective of multi-layer network. Reliability Eng. Syst. Safety (2022). https://doi.org/10.1016/j.ress.2021.108161

Yu, W., Wang, T., Zheng, Y., Chen, J.: Parameter selection and evaluation of robustness of nanjing metro network based on supernetwork. IEEE ACCESS (2019). https://doi.org/10.1109/access.2019.2917678

Zhang, J., Huang, D., You, Q., Kang, J., Shi, M., Lang, X.: Evaluation of emergency evacuation capacity of urban metro stations based on combined weights and TOPSIS-GRA method in intuitive fuzzy environment. Int. J. Disaster Risk Reduct. **95**(Suppl C), 103864 (2023). https://doi.org/10.1016/j.ijdrr.2023.103864

Zhang, J., Min, Q., Zhou, Y., Cheng, L.: Vulnerability assessments of urban rail transit networks based on extended coupled map lattices with evacuation capability. Reliab. Eng. Syst. Saf. **243**, 109826 (2024). https://doi.org/10.1016/j.ress.2023.109826

Zhang, L., Lu, J., & Lei, D.: Vulnerability analysis of bus-metro composite network based on complex network and spatial information embedding(Article). Dongnan Daxue Xuebao (Ziran Kexue Ban)/J. Southeast Univ. https://doi.org/10.3969/j.issn.1001-0505.2019.04.022

Jie li is an associate professor in the College of Civil Engineering, Hunan University. Her main research interests include multi-modal transportation system resilience assessment and improvement, electric vehicle health monitoring and charging infrastructure planning, and traffic safety and driving behavior.

Ying Luo is a postgraduate student in the College of Civil Engineering, Hunan University. Her research focuses on the resilience analysis and improvement strategies of urban rail transit networks under urban flooding scenarios, based on the cascading failure model.

Jianghang Ou is a postgraduate student in the College of Civil Engineering, Hunan University. His research interests mainly focus on the resilience assessment of urban multimodal transportation networks and resilience enhancement strategies, with particular attention to the impact of urban rainfall on multimodal transportation network resilience.

Suhua Zhou is an associate professor in the College of Civil Engineering at Hunan University. He is primarily engaged in research on digital construction, operation and maintenance, and disaster prevention and mitigation in geotechnical engineering, with a specific focus on disaster prevention and mitigation in mountainous areas and urban infrastructure.

Chaoru Lu is currently an associate professor of smart mobility at the Department of Civil Engineering and Energy Technology, Oslo Metropolitan University. His research work mainly lies in intelligent transport system, traffic flow theory, autonomous vehicle, and transport electrification.

Yun Zhou is the vice dean of the College of Civil Engineering at Hunan University. His main research areas are artificial intelligence structural health monitoring, prefabricated concrete structures, and new structural testing technologies.